

Iridium-related complexes in Czochralski-grown β -Ga₂O₃

Jacob R. Ritter,¹ Kelvin G. Lynn,^{1,2} and Matthew D. McCluskey^{1,*}

¹Dept. of Physics and Astronomy, Washington State University, Pullman, WA, USA 99164-2814

²Center for Materials Research, Washington State University, Pullman, WA, USA 99164-2711

ABSTRACT

Gallium oxide is a promising semiconductor for its potential as a material in the field of power electronics. The effects of iridium impurities on undoped, Mg-doped, and Ca-doped gallium oxides were investigated with IR spectroscopy. In undoped and Ca-doped β -Ga₂O₃, IR peaks at 3313, 3450, and 3500 cm⁻¹ are tentatively assigned to O–H bond stretching modes of IrH complexes. Mg, Ca, and Fe doped samples show an Ir⁴⁺ electronic transition feature at 5148 cm⁻¹. By measuring the strength of this feature versus photoexcitation, the Ir^{3+/4+} donor level was determined to lie 2.2-2.3 eV below the conduction band minimum. Ga₂O₃:Mg also has a range of sidebands between 5100 and 5200 cm⁻¹, attributed to IrMg pairs. Polarized IR measurements show that the 5248 cm⁻¹ peak is anisotropic, weakest for light polarized along the **c** axis, consistent with Lenyk *et al.* [J. Appl. Phys. **125**, 045703 (2019)].

I. INTRODUCTION

In the field of power electronics, gallium oxide (Ga₂O₃) shows promise for its wide bandgap (4.5-4.8 eV) and impressively high breakdown field.¹⁻³ The most stable phase, β -Ga₂O₃, is inexpensive and straightforward to grow as single crystals.⁴⁻⁷ Nominally undoped β -Ga₂O₃ crystals are predominately *n*-type. Although acceptor doping has failed to create *p*-type material with good hole conduction, certain acceptors have been found to create semi-insulating β -Ga₂O₃,

* Email: mattmcc@wsu.edu

which could be useful in power electronic devices.⁸⁻¹¹ In previous work, we investigated magnesium and calcium as two such potential acceptors.^{12,13} While Mg produces semi-insulating material (resistances in the $\sim 100\text{ G}\Omega$ range), Ca-doped samples are more insulating than undoped Ga_2O_3 ($\sim 10\text{ M}\Omega$ compared to $\sim 10\text{ K}\Omega$) but lightly *n*-type.

Because iridium incorporation is often part of the growth process due to iridium crucibles, it is important to study the effect of this impurity. Iridium is a deep double donor that compensates acceptors.¹² An IR absorption peak with multiple sidebands was attributed to an electronic transition from the Ir^{4+} ground state to an excited *d*-orbital. The primary Ir^{4+} peak is at 5148 cm^{-1} . Hydrogen, a common impurity, passivates acceptors to form MgH and CaH complexes with O–H bond-stretching frequencies at 3492 and 3441 cm^{-1} , respectively.^{12,13} In both undoped and calcium-doped $\beta\text{-Ga}_2\text{O}_3$ we observed unidentified hydrogen peaks at 3313 , 3450 , and 3500 cm^{-1} .

In this work we used secondary ion mass spectrometry (SIMS) and IR measurements to identify these peaks as iridium related; specifically, O–H bond-stretching vibrational modes associated with an IrH complex. We also show evidence that the previously identified Ir^{4+} peak is due to isolated iridium while its neighboring sidebands are due to IrMg pairs.

II. EXPERIMENTAL METHODS

$\beta\text{-Ga}_2\text{O}_3$ single crystals were grown from a high purity gallium oxide powder (99.999%) from GFI Advanced Technologies. The boules were grown from a 1 kg charge using the Czochralski (CZ) method in an iridium crucible. The primary dopants investigated in this work (Mg, Ca) were added to the charge during growth, while hydrogen and deuterium impurities

were added later. All samples grown this way cleaved in the a -plane (100) and any optical measurements were taken with the incident light normal to the (100) surface unless specified. A CZ-grown β -Ga₂O₃:Fe sample with $\langle 010 \rangle$ orientation was purchased from the MTI Corporation as a point of reference.

Hydrogen and deuterium were incorporated into the sample via diffusion, by sealing the sample in a silica ampoule with the desired ratio of hydrogen and deuterium gas at $\frac{1}{2}$ atm total pressure. The samples were then furnace annealed and water quenched to room temperature. Mg- and Ca-doped samples were annealed at 860°C for 3.5 hr and undoped samples were annealed at 820°C for 2 hr.

IR transmission spectra were collected with a Bomem DA8 vacuum Fourier transform infrared (FTIR) spectrometer at 10 K. The system contains a KBr beamsplitter, silicon carbide light source, and InSb detector. The instrumental resolution was 0.5 cm⁻¹. The IR beam was unpolarized unless noted otherwise.

SIMS analysis was performed by the Evans Analytical Group (EAG) on deuterated samples of undoped, Ca-doped, and Mg-doped β -Ga₂O₃ to a depth of 3 μ m. We acquired profiles of deuterium, silicon, magnesium, calcium, and iridium concentrations. D and Si were calibrated from implant standards and accurate to 30%, while Ir, Mg, and Ca were uncalibrated and estimated by EAG to only be accurate to a factor of 3. The primary ions for the calibrated concentrations were Cs⁺ and the primary ions for uncalibrated concentrations were O₂⁺. Lenyk et al.²⁰ established a calibration for Ir⁴⁺ concentration given by $N = (2.4 \times 10^{18} \text{ cm}^{-2})\alpha$, where α is the absorption coefficient (cm⁻¹) of the room-temperature Ir⁴⁺ peak for light polarized along the a axis. From the peak height in a Ga₂O₃:Mg sample, the calibration indicates an Ir⁴⁺ concentration in the mid-10¹⁸ cm⁻³ range (Supplementary Material). This value is an order of magnitude larger

than the SIMS estimates (Table 1). Therefore, the absolute concentrations for Ir should not be taken as accurate.

III. IRIIDIUM-HYDROGEN PEAKS

As reported previously¹², IR spectra of hydrogen-annealed undoped Ga₂O₃ presented hydrogen related peaks at 3313, 3437, 3450, and 3500 cm⁻¹ (Fig. 1). Deuterating the sample yields corresponding peaks with an isotopic frequency shift of 1.35, comparable to O–H and O–D shifts observed in other oxide semiconductors (Fig. 2).^{14,15} The 3437 cm⁻¹ peak has been previously identified as a gallium vacancy decorated by two hydrogen atoms, or V_{Ga}2H,¹⁶ but the remaining peaks were unassigned.

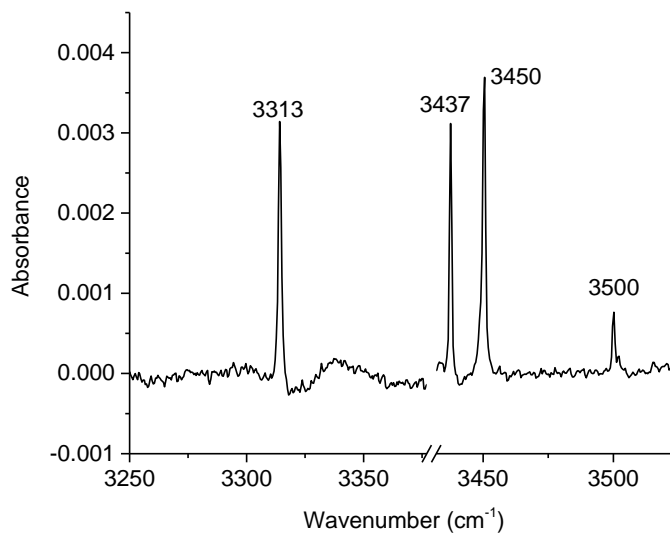


Figure 1: IR spectrum of undoped gallium oxide (1.2 mm thick) annealed in hydrogen. The 3437 cm⁻¹ peak is due to a vacancy-hydrogen complex, while the other peaks are attributed to IrH complexes.

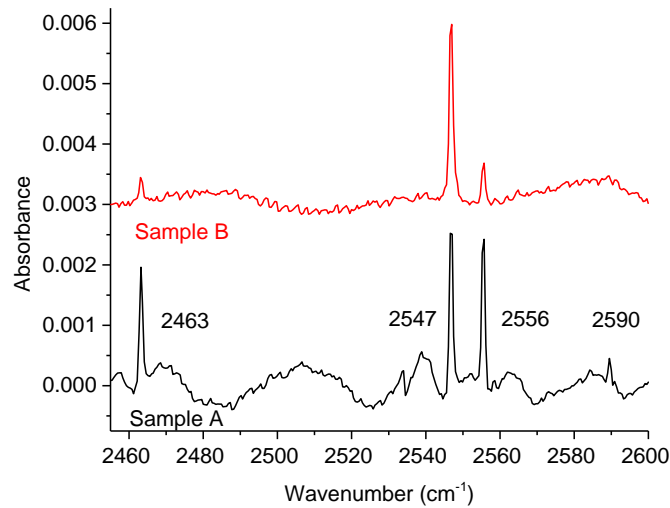


Figure 2: IR spectra of two samples of deuterium annealed, undoped gallium oxide. Both samples are from the same boule. Sample A has an Ir concentration roughly 4 times that of Sample B. The thickness of A and B is 1-2 mm and 1.4 mm respectively. Spectra are offset for clarity.

D-annealing of another crystal taken from the same boule presented the $V_{\text{Ga}2\text{D}}$ peak but had much lower intensities for the $3313/2463\text{ cm}^{-1}$, $3450/2556\text{ cm}^{-1}$, and $3500/2590\text{ cm}^{-1}$ peaks (Fig. 2). Inspection of the growth conditions of the two samples revealed that the sample with the strong 3450 cm^{-1} peak was taken from a region much nearer the seed crystal holder, which was made from iridium. This led to a suspicion that the peak was an iridium-related feature. SIMS analysis was used to compare the iridium concentrations between the two samples (Table 1). The crystal with the strong $3450/2456\text{ cm}^{-1}$ peak contained roughly four times as much iridium than the sample with the weaker peak. From this correlation we tentatively assign the 3313 , 3450 , and 3500 cm^{-1} peaks to O–H stretching modes associated with iridium-hydrogen complexes.

This is the author's peer reviewed, accepted manuscript. However, the online version of record will be different from this version once it has been copyedited and typeset.
PLEASE CITE THIS ARTICLE AS DOI: 10.1063/1.5129781

| | D | Si | Ir | Mg | Ca |
|--|----------------------|----------------------|----------------------|----------------------|----------------------|
| Detection limit | 8.0×10^{14} | 1.0×10^{15} | 5.0×10^{15} | 5.0×10^{14} | 5.0×10^{13} |
| Undoped Ga ₂ O ₃ (A) | 1.8×10^{15} | 5.1×10^{16} | 4.6×10^{16} | 1.9×10^{15} | - |
| Undoped Ga ₂ O ₃ (B) | 1.5×10^{15} | 6.8×10^{16} | 1.1×10^{16} | - | - |
| Mg-doped Ga ₂ O ₃ | 1.4×10^{18} | 1.7×10^{17} | 7.1×10^{16} | 7.4×10^{18} | - |
| Ca-doped Ga ₂ O ₃ | 5.5×10^{15} | 3.5×10^{16} | 2.3×10^{17} | - | 1.0×10^{16} |

Table 1: SIMS analysis of impurity concentrations (cm^{-3}) for Mg-doped, Ca-doped, and unintentionally doped Ga₂O₃, all annealed in deuterium. Note that the concentrations for Ir, Mg, and Ca are uncalibrated.

The IrH and V_{Ga}2H peaks were also identified in deuterated calcium-doped Ga₂O₃, as well as the previously identified Ca-related O–H bond stretching mode at $3441/2557 \text{ cm}^{-1}$ (Fig. 3).¹³ In Mg-doped Ga₂O₃ only the MgH complex at 3492 cm^{-1} is observed despite comparable levels of iridium, with no evidence of either the V_{Ga}2H or the IrH complexes (Fig. 3).

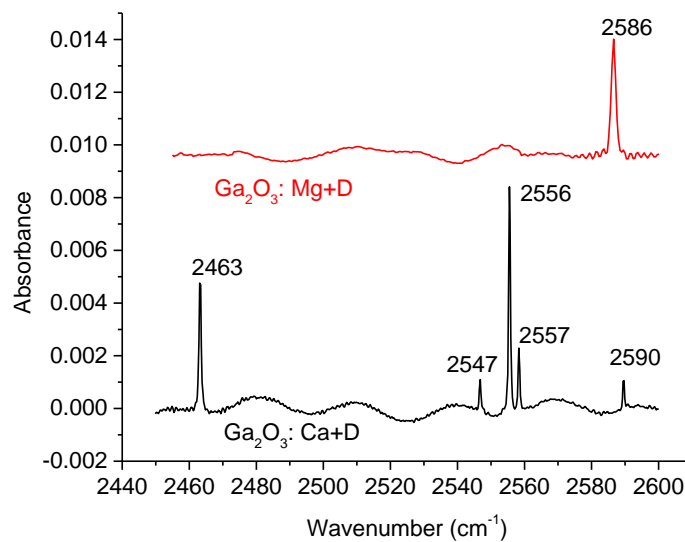


Figure 3: IR spectra of deuterated Ga₂O₃:Mg (top) and Ga₂O₃:Ca (bottom). 2586 cm^{-1} is a peak for a MgD O–D stretching mode in Ga₂O₃:Mg and 2556 cm^{-1} is a peak for a CaD complex in Ga₂O₃:Ca. Spectra offset for clarity. Sample thicknesses were 1-2 mm.

IV. Ir⁴⁺ ELECTRONIC TRANSITIONS

Mg-doped Ga₂O₃ samples show a strong IR absorption peak at 5148 cm⁻¹ and a large number of smaller neighboring peaks from 5090-5190 cm⁻¹ (Fig. 4, Table 2).

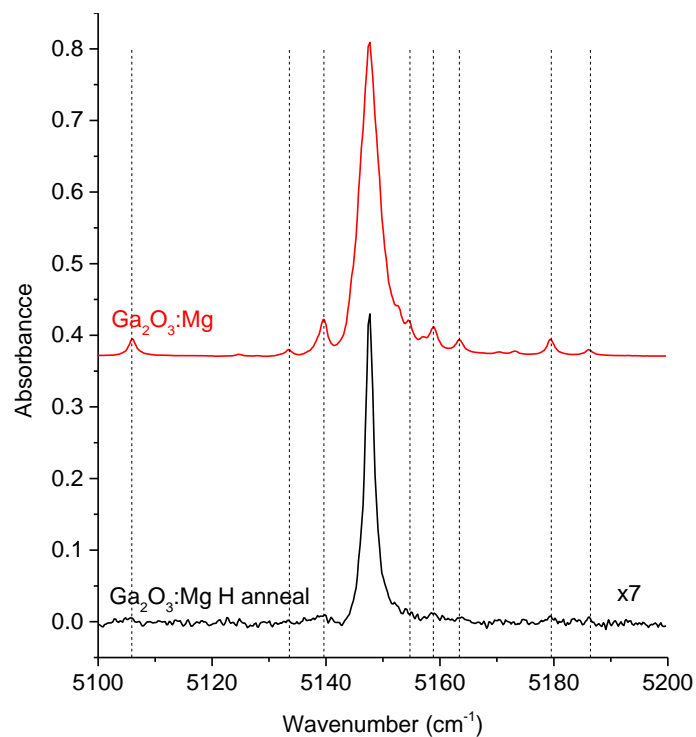


Figure 4: IR spectra of Mg-doped gallium oxide, as-grown (2.4 mm thick) and hydrogen annealed (1.6 mm thick). The hydrogen-annealed sample is scaled for comparison. Spectra are offset for clarity.

| Ir ⁴⁺ peak positions (cm ⁻¹) | Relative height |
|---|-----------------|
| 5092.4 | 0.015 |
| 5106.0 | 0.054 |
| 5124.6 | 0.005 |
| 5128.0 | 0.001 |
| 5133.5 | 0.021 |
| 5139.6 | 0.112 |
| 5147.6 (primary) | 1.000 |
| 5152.6 | 0.020 |
| 5154.4 | 0.034 |
| 5157.2 | 0.018 |
| 5158.8 | 0.060 |
| 5163.4 | 0.040 |
| 5170.3 | 0.008 |

| | |
|--------|-------|
| 5173.2 | 0.010 |
| 5179.4 | 0.053 |
| 5185.2 | 0.018 |

Table 2: List of peak energies for Ir⁴⁺ in Ga₂O₃:Mg (see Fig. 4).

Similarly sharp absorption bands in this region have previously been attributed to an electronic transition of Ir⁴⁺ in other oxide crystals.^{17–19} Accordingly, we have assigned the primary peak at 5148 cm⁻¹ to a transition from the Ir⁴⁺ ground state to an excited *d*-orbital.^{12,20} Undoped Ga₂O₃ samples that have similar concentrations of iridium (Table 1) do not show evidence of these features, presumably because the iridium is in the form of Ir³⁺, which is not IR active for electronic transitions. Magnesium accepts an electron from the iridium donor, creating the IR-active Ir⁴⁺. Further supporting this idea, the magnesium acceptors can be passivated to be neutral through hydrogen annealing. The neutral complexes can no longer be compensated by iridium donors, and so the majority of iridium in the crystal has the form of Ir³⁺. As a result, hydrogen annealing Ga₂O₃:Mg greatly suppresses the Ir⁴⁺ peak (Fig. 4). The width of the peak (FWHM) in as-grown and hydrogen-annealed Ga₂O₃:Mg is 4.0 and 1.8 cm⁻¹ respectively.

First-principles calculations assigned a 2.25 eV energy onset for the transition from the Ir_{Ga} level to the conduction band in Ga₂O₃:Mg.¹² In the present work, we exposed a hydrogen-annealed Ga₂O₃:Mg sample to incrementally shorter wavelength light emitting diodes (LEDs). The LEDs had a spectral width of 20-30 nm, were operated at a current of 0.8 A, and caused a sample temperature increase of <1.0 K. Photon energies above 2.3 eV increase the Ir⁴⁺ peak area significantly, as the photon excites an electron from Ir³⁺ to the conduction band to create more Ir⁴⁺ (Fig. 5). When plotting the peak intensity vs excitation energy, the threshold of activation for this transition falls between 2.2 and 2.3 eV (Fig. 6). This finding agrees with the calculated 2.25 eV energy onset.

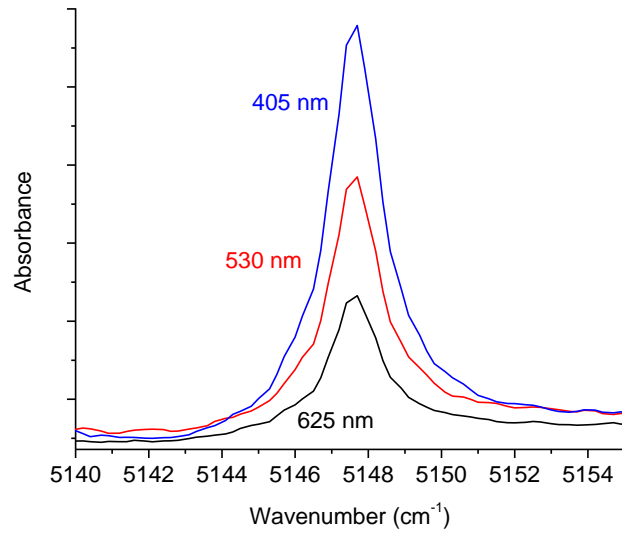


Figure 5: IR spectra of H-annealed $\text{Ga}_2\text{O}_3:\text{Mg}$. When exposed to photons of increasing energy, more iridium in the Ir^{3+} state is excited to Ir^{4+} , increasing the size of the 5148 cm^{-1} Ir^{4+} peak.

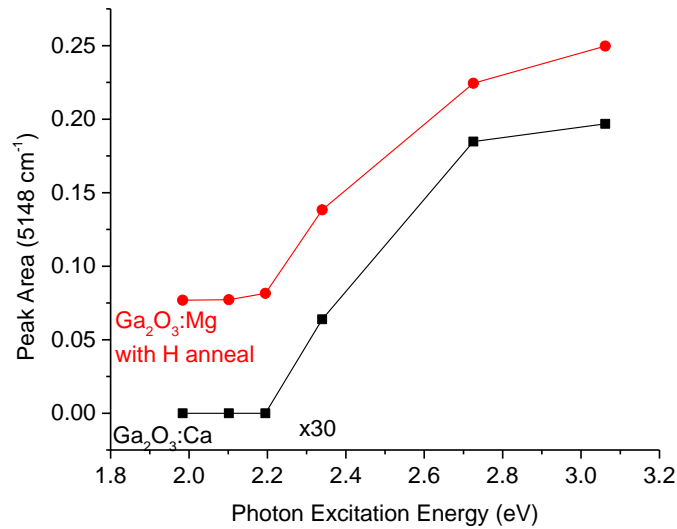


Figure 6: Plot of the 5148 cm^{-1} peak versus excitation photon energy for $\text{Ga}_2\text{O}_3:\text{Ca}$ (squares) and H-annealed $\text{Ga}_2\text{O}_3:\text{Mg}$ (circles). Sequential exposures of increasingly higher energy light show that the threshold for exciting an electron from the Ir^{3+} level to the conduction band minimum occurs between 2.2 and 2.3 eV.

We performed similar experiments on calcium-doped gallium oxide. Even though the IR spectra for $\text{Ga}_2\text{O}_3:\text{Ca}$ initially showed no evidence of an Ir^{4+} feature, photon excitation produced

a comparable threshold for a Ir^{4+} peak to appear (Fig. 6). This provides further evidence that that the energy level for iridium in Ga_2O_3 is 2.25 eV below the conduction band minimum.

A $\text{Ga}_2\text{O}_3:\text{Fe}$ sample with (010) surface orientation also shows this peak, and the feature can be greatly enhanced with sufficient photon excitation (Fig. 7). Iron can act as a deep acceptor in Ga_2O_3 , but because the iron level is not as deep as the Ir level, it is surprising to see evidence of the Ir^{4+} transition¹¹. The Fe-doped sample presumably contains an acceptor complex with a level that lies below the $\text{Ir}^{3+/4+}$ donor level.

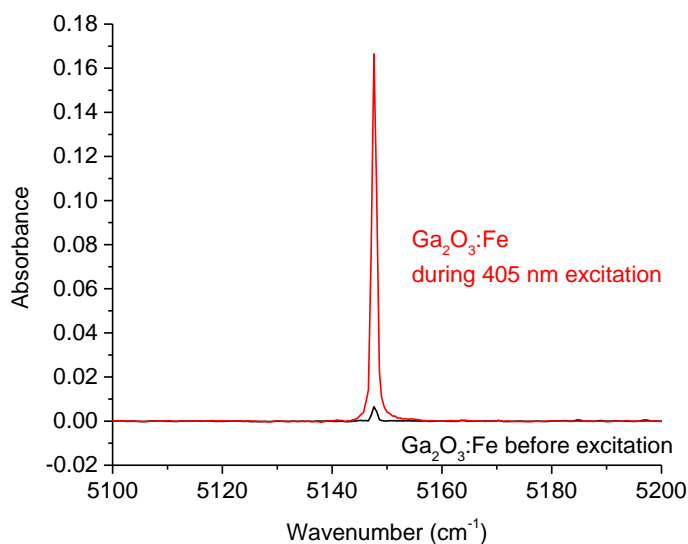


Figure 7: IR spectra of the 5148 cm^{-1} Ir^{4+} peak in $\text{Ga}_2\text{O}_3:\text{Fe}$ (0.35 mm thick) before (black) and during (red) excitation with 405 nm light.

While the primary peak at 5148 cm^{-1} is assigned to an Ir^{4+} transition, there is evidence that the neighboring sidebands arise from more complex defects. When a $\text{Ga}_2\text{O}_3:\text{Mg}$ sample was excited by a series of increasingly energetic photons, there was no change in the intensity of the 5148 cm^{-1} peak. This is because all of the iridium is already in the Ir^{4+} state. Therefore, there are no Ir^{3+} states to excite.

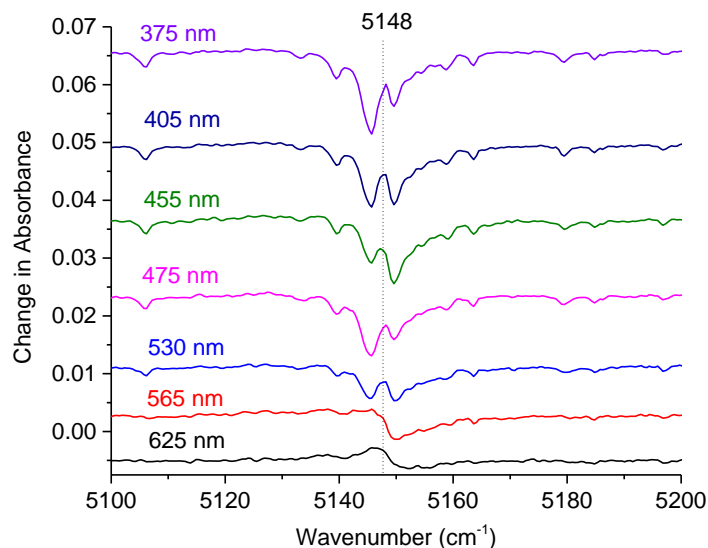


Figure 8: IR subtraction spectra of $\text{Ga}_2\text{O}_3:\text{Mg}$ (2.4 mm thick) exposed to LEDs. Each spectrum is subtracted against an IR spectrum taken before the sample was exposed to light. Even though there was no change in the primary 5148 cm^{-1} peak, the subtraction spectra reveal that there are small changes in the absorbance of all of the sideband features, suggesting that the sidebands and primary peak come from different defects. Spectra are offset vertically for clarity.

However, a subtraction spectrum reveals that the sidebands decrease in absorbance with higher energy excitation photons, implying that the sidebands arise from different centers than the primary peak (Fig. 8). Furthermore, while the 5148 cm^{-1} peak can be enhanced in other samples, like $\text{Ga}_2\text{O}_3:\text{Ca}$ and $\text{Ga}_2\text{O}_3:\text{Fe}$, both also grown with iridium, the sidebands only arise in the presence of magnesium (Fig. 9). Because of this, we posit that the sideband peaks are due to iridium-magnesium pairs, where the Ir^{4+} transition is perturbed by a neighboring Mg^- . The slight decrease in absorbance suggests that the excitation puts some of the iridium into the Ir^{3+} state, perhaps by neutralizing a magnesium acceptor via charge transfer ($\text{Ir}^{4+}\text{Mg}^- \rightarrow \text{Ir}^{3+}\text{Mg}^0$).

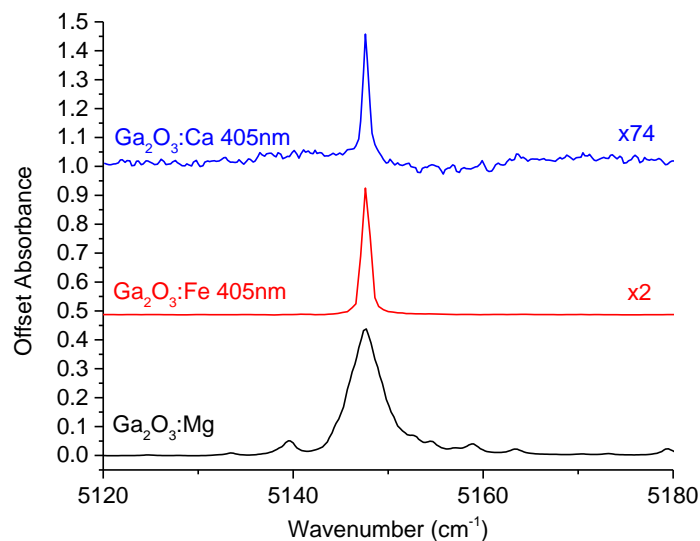


Figure 9: IR spectra of Ir^{4+} in Mg, Fe, and Ca doped gallium oxide. Thicknesses are 2.4, 0.35, and 1.2 mm respectively. The Mg doped sample has sidebands that are not present in samples without Mg. The larger width of the $\text{Ga}_2\text{O}_3:\text{Mg}$ Ir^{4+} peak is at least partially due to sidebands underneath the primary peak (Fig. 8). Spectra have been offset vertically and scaled for clarity.

Comparison of $\text{Ga}_2\text{O}_3:\text{Mg}$ with and without a hydrogen anneal shows that hydrogen annealing suppresses the Ir^{4+}Mg peaks more than the primary Ir^{4+} peak (Fig. 4). While the primary peak is reduced by a factor of 7, the sidebands are smaller by a factor of ~ 30 and barely visible at all. This loss suggests that as the Fermi level rises, the Ir^{4+}Mg level is occupied before the Ir^{4+} level is. The occupied levels, Ir^{3+}Mg and Ir^{3+} , have no IR signature. Therefore, the Ir^{4+}Mg level is below the Ir^{4+} level.

Polarization experiments show that the Ir^{4+} peak and sidebands have preferred directions of excitation. For a (100) oriented Mg-doped sample a linear polarizer was inserted into the beam path such that $\Theta = 0^\circ$ corresponds to light polarized along the **b** axis. As shown in Fig. 10, the Ir^{4+} peak is strongest when the incident light is polarized along the **b** axis and weakest when polarized along the **c** axis. Similarly, for the Fe-doped (010) oriented sample, the peak is strongest with incident light polarized along the **a** axis and weakest along the **c** axis (Fig. 10).

These results suggest that while the $\text{Ir}^{3+/4+}$ transition is significantly less probable along the \mathbf{c} axis it is not disallowed entirely, in agreement with the findings of Lenyk *et al.*²⁰ More investigation is needed to understand the origin of this anisotropy.

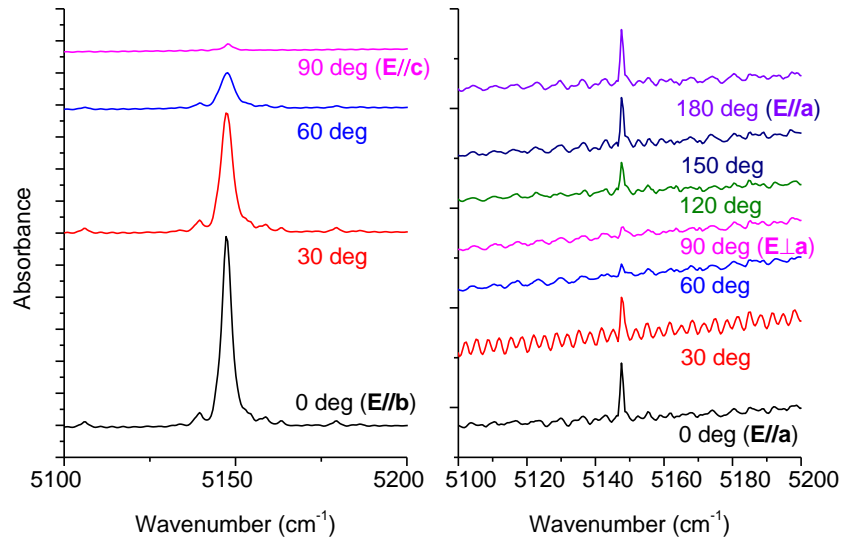


Figure 10: Polarized IR spectra for $\text{Ga}_2\text{O}_3:\text{Mg}$ (left) and $\text{Ga}_2\text{O}_3:\text{Fe}$ (right). For the Mg-doped spectrum light is incident to the (100) plane and for the Fe-doped spectrum light is incident to the (010) plane.

V. CONCLUSIONS

In conclusion, iridium incorporation in gallium oxide leads to several defect complexes. In both undoped and Ca-doped Ga_2O_3 annealed in hydrogen, O–H vibrational modes at 3313, 3450, and 3500 cm^{-1} were tentatively attributed to IrH complexes. In general, donor-hydrogen complexes do not form in oxide semiconductors because a positively charged donor will repel a proton. Because Ir is a deep donor, however, it has a neutral charge state (Ir^{3+}) in n -type material. It is conceivable that the higher Pauling electronegativity of Ir (2.2) as compared to Ga (1.6) may result in an increase in negative charge around the defect that makes this site energetically favorable for a proton.

In Mg-doped Ga₂O₃ there is an electronic transition related to Ir⁴⁺ at 5148 cm⁻¹, as well as numerous smaller transition peaks ranging from 5090-5190 cm⁻¹. Our experimental results concur with first-principles calculations that place the Ir donor level 2.25 eV below the conduction-band minimum. Since smaller transition peaks can only be seen in Mg-doped Ga₂O₃, we assign them to iridium-magnesium pairs, each energetically different based on the specific site of the magnesium neighbor. The strength of the Ir⁴⁺ peak is weakest for light polarized along the **c** axis.²⁰

SUPPLEMENTARY MATERIAL

See supplementary material for SIMS profiles, spectra of illuminated Ga₂O₃:Mg, and spectra of Ga₂O₃:Mg at several temperatures.

ACKNOWLEDGMENTS

The authors acknowledge the help of Muad Saleh and Peter Dickens at the Center for Materials Research at WSU for crystal growth. This research was supported by the U.S. Department of Energy, Office of Basic Energy Sciences, Division of Materials Science and Engineering under Award No. DE-FG02-07ER46386.

- ¹ M. Higashiwaki, K. Sasaki, A. Kuramata, T. Masui, and S. Yamakoshi, *Phys. Status Solidi A* **211**, 21 (2014).
- ² K. Sasaki, A. Kuramata, T. Masui, E.G. Villora, K. Shimamura, and S. Yamakoshi, *Appl. Phys. Express* **5**, 035502 (2012).
- ³ N. Ueda, H. Hosono, R. Waseda, and H. Kawazoe, *Appl. Phys. Lett.* **71**, 933 (1997).
- ⁴ K. Irmscher, Z. Galazka, M. Pietsch, R. Uecker, and R. Fornari, *J. Appl. Phys.* **110**, 063720 (2011).
- ⁵ S. Geller, *J. Chem. Phys.* **33**, 676 (1960).
- ⁶ E.G. Villora, K. Shimamura, Y. Yoshikawa, K. Aoki, and N. Ichinose, *J. Cryst. Growth* **270**, 420 (2004).
- ⁷ Z. Galazka, R. Uecker, D. Klimm, K. Irmscher, M. Naumann, M. Pietsch, A. Kwasniewski, R. Bertram, S. Ganschow, and M. Bickermann, *ECS J. Solid State Sci. Technol.* **6**, Q3007 (2017).
- ⁸ Z. Galazka, K. Irmscher, R. Uecker, R. Bertram, M. Pietsch, A. Kwasniewski, M. Naumann, T. Schulz, R. Schewski, D. Klimm, and M. Bickermann, *J. Cryst. Growth* **404**, 184 (2014).
- ⁹ T. Onuma, S. Fujioka, T. Yamaguchi, M. Higashiwaki, K. Sasaki, T. Masui, and T. Honda, *Appl. Phys. Lett.* **103**, 041910 (2013).
- ¹⁰ B.E. Kananen, L.E. Halliburton, E.M. Scherrer, K.T. Stevens, G.K. Foundos, K.B. Chang, and N.C. Giles, *Appl. Phys. Lett.* **111**, 072102 (2017).
- ¹¹ M.E. Ingebrigtsen, J.B. Varley, A.Yu. Kuznetsov, B.G. Svensson, G. Alfieri, A. Mihaila, U. Badstübner, and L. Vines, *Appl. Phys. Lett.* **112**, 042104 (2018).
- ¹² J.R. Ritter, J. Huso, P.T. Dickens, J.B. Varley, K.G. Lynn, and M.D. McCluskey, *Appl. Phys. Lett.* **113**, 052101 (2018).
- ¹³ J.R. Ritter, K.G. Lynn, and M.D. McCluskey, *Proc SPIE* 10919 (2019).
- ¹⁴ M.D. McCluskey, S.J. Jokela, K.K. Zhuravlev, P.J. Simpson, and K.G. Lynn, *Appl. Phys. Lett.* **81**, 3807 (2002).
- ¹⁵ W. Ulrici, M. Czapalla, and M. Seifert, *Phys. Status Solidi B* **210**, (1998).
- ¹⁶ P. Weiser, M. Stavola, W.B. Fowler, Y. Qin, and S. Pearton, *Appl. Phys. Lett.* **112**, 232104 (2018).

This is the author's peer reviewed, accepted manuscript. However, the online version of record will be different from this version once it has been copyedited and typeset.

PLEASE CITE THIS ARTICLE AS DOI: 10.1063/1.5129781

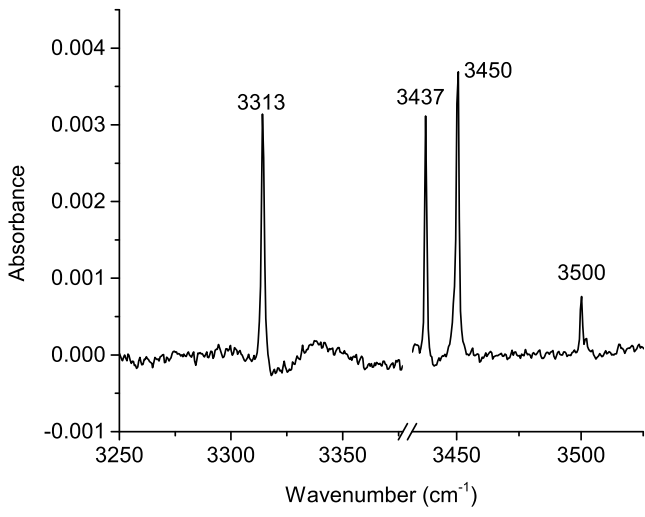
¹⁷ O.F. Schirmer, A. Forster, H. Hesse, M. Wohlecke, and S. Kapphan, *J. Phys. C Solid State Phys.* **17**, 1321 (1984).

¹⁸ B. Andlauer, J. Schneider, and W. Tolksdorf, *Phys. Status Solidi B* **73**, 533 (1976).

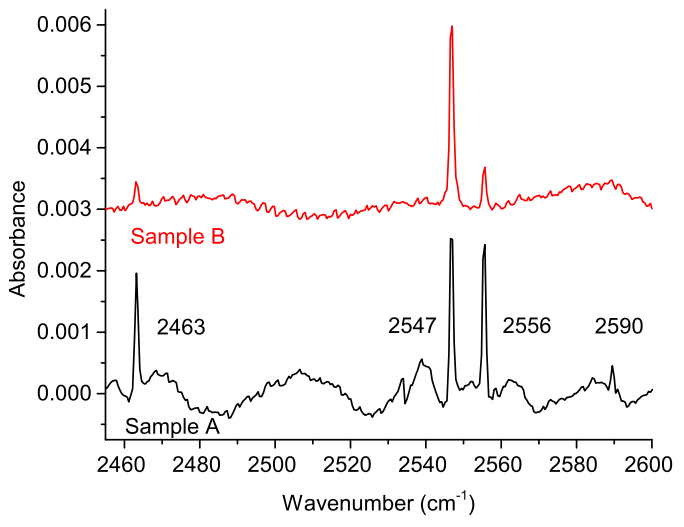
¹⁹ T.A. Keiderling, P.J. Stephens, S.B. Piepho, J.L. Slater, and P.N. Schatz, *Chem. Phys.* **11**, 343 (1975).

²⁰ C.A. Lenyk, N.C. Giles, E.M. Scherrer, B.E. Kananen, L.E. Halliburton, K.T. Stevens, G.K. Foundos, J.D. Blevins, D.L. Dorsey, and S. Mou, *J. Appl. Phys.* **125**, 045703 (2019).

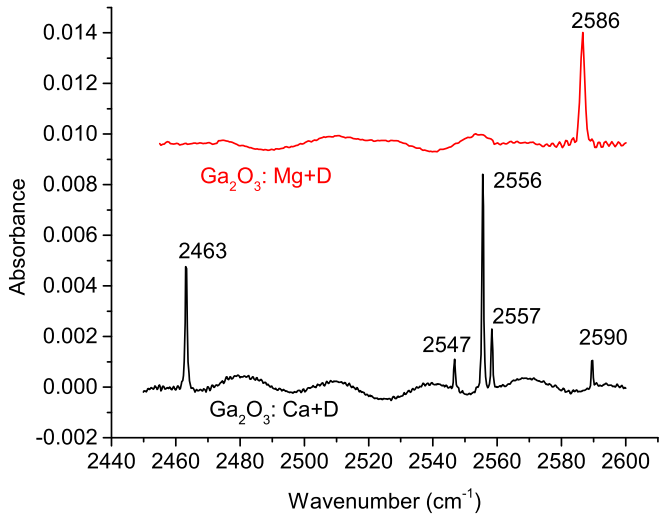
This is the author's peer reviewed, accepted manuscript. However, the online version of record will be different from this version once it has been copyedited and typeset.
PLEASE CITE THIS ARTICLE AS DOI: 10.1063/1.5129781



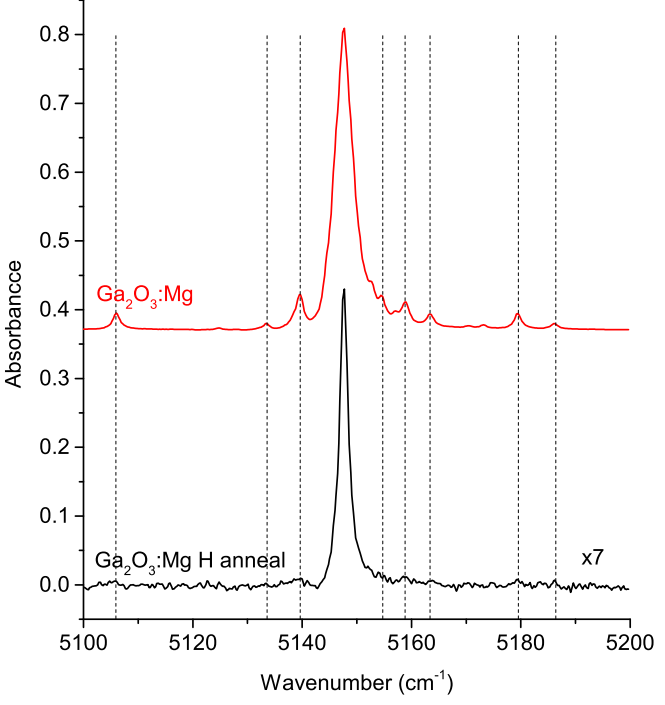
This is the author's peer reviewed, accepted manuscript. However, the online version of record will be different from this version once it has been copyedited and typeset.
PLEASE CITE THIS ARTICLE AS DOI: 10.1063/1.5129781



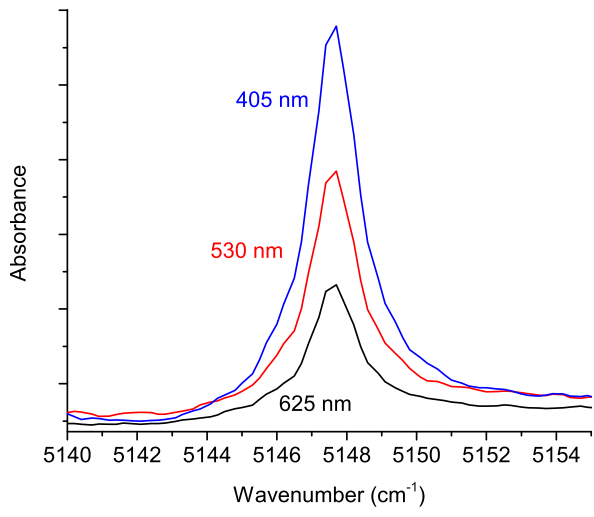
This is the author's peer reviewed, accepted manuscript. However, the online version of record will be different from this version once it has been copyedited and typeset.
PLEASE CITE THIS ARTICLE AS DOI: 10.1063/1.5129781



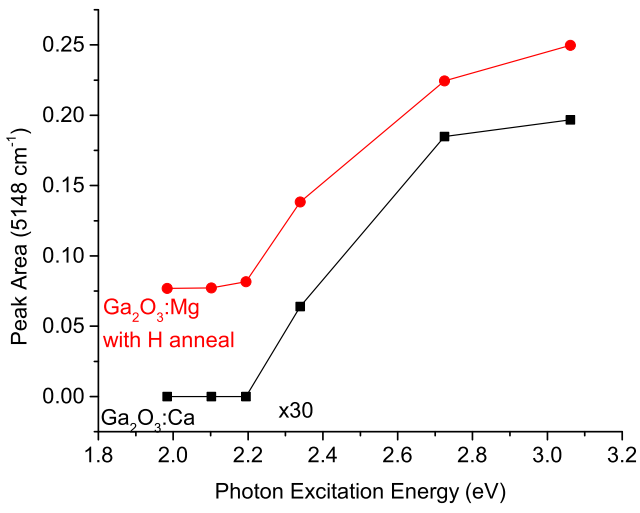
This is the author's peer reviewed, accepted manuscript. However, the online version of record will be different from this version once it has been copyedited and typeset.
PLEASE CITE THIS ARTICLE AS DOI: 10.1063/1.5129781



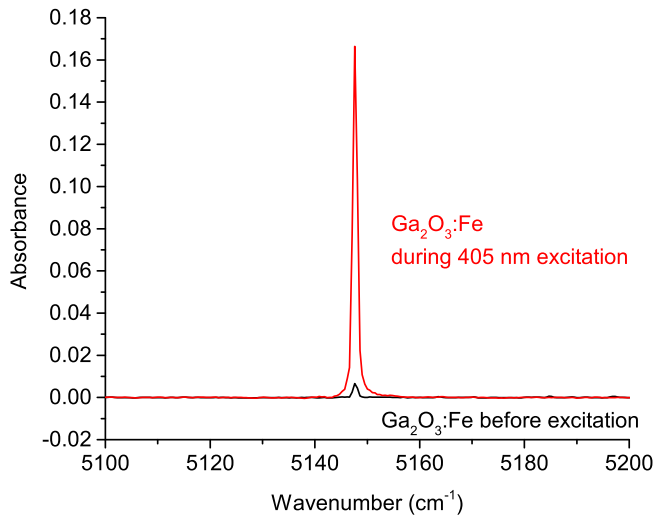
This is the author's peer reviewed, accepted manuscript. However, the online version of record will be different from this version once it has been copyedited and typeset.
PLEASE CITE THIS ARTICLE AS DOI: 10.1063/1.5129781



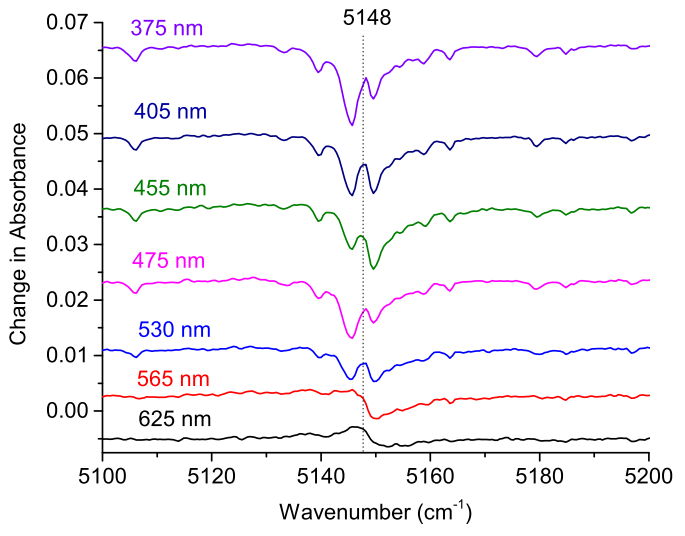
This is the author's peer reviewed, accepted manuscript. However, the online version of record will be different from this version once it has been copyedited and typeset.
PLEASE CITE THIS ARTICLE AS DOI: 10.1063/1.5129781



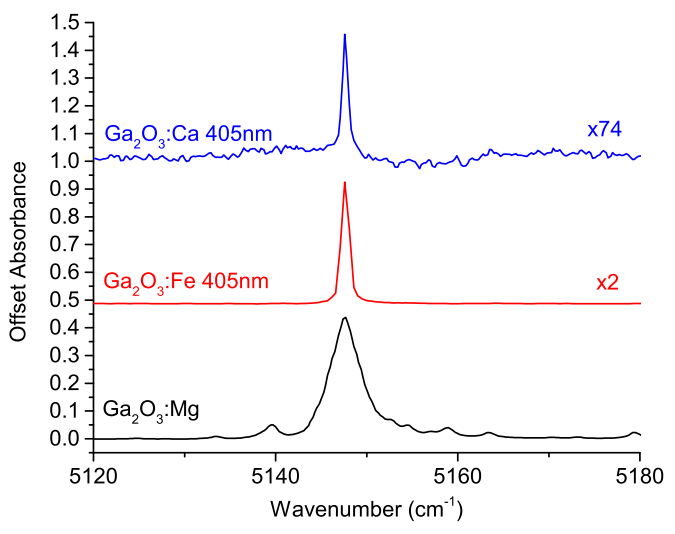
This is the author's peer reviewed, accepted manuscript. However, the online version of record will be different from this version once it has been copyedited and typeset.
PLEASE CITE THIS ARTICLE AS DOI: 10.1063/1.5129781



This is the author's peer reviewed, accepted manuscript. However, the online version of record will be different from this version once it has been copyedited and typeset.
PLEASE CITE THIS ARTICLE AS DOI: 10.1063/1.5129781



This is the author's peer reviewed, accepted manuscript. However, the online version of record will be different from this version once it has been copyedited and typeset.
PLEASE CITE THIS ARTICLE AS DOI: 10.1063/1.5129781



This is the author's peer reviewed, accepted manuscript. However, the online version of record will be different from this version once it has been copyedited and typeset.
PLEASE CITE THIS ARTICLE AS DOI: 10.1063/1.5129781

